

# Pattern wiggling investigation of self-aligned double patterning for 2x nm node NAND Flash and beyond

\*1 You-Yu Lin, \*1 Chun-Chi Chen, \*1 Chia-Yu Li, \*2 Zih-Song Wang, \*3 Ching-Hua Chen  
\*1 Powerchip Technology Corp., No. 12, Li-Hsin 1st Rd., Hsinchu, Taiwan, R. O. C.  
\*2 Institute of Electronics Engineering, National Tsing Hua University  
\*3 Department of Materials Science and Engineering, National Chiao Tung University

## Abstract

Double patterning technology (DPT) has been identified as the extension of optical photolithography technologies to 3x nm half-pitch and below to fill in the gap between Immersion and EUV lithography. Self-aligned double patterning (SADP) technology utilized mature process to reduce risk and faster time to support the continuation of Moore's Law. As for the SADP process, the suitable hard mask (HM) material as following core pattern selection is quite important. Usually, the severe pattern deformation –wiggling, is easy to happen as the line/space patterns scaled down to below 35nm, and it ultimately prevents the successful pattern transfer. In this paper, using the amorphous carbon as HM, it was found that wiggling was caused by serious chemical side-etch during SADP dry etch process. However, an effective of advanced carbon material with high etch selectivity and low etch rate by appropriate film modification can be successful in SADP without wiggling side effect for 2x nm node NAND Flash application. This extraordinary HM can be considered as a potential choice for SADP process continual performing.

Keywords : wiggling, SADP(Self-aligned double patterning), amorphous carbon, etch selectivity.

## 1. Introduction

To aim goal of 2X nm half-pitch patterning, EUVL is designed as the must in lithography to continuous scaling extension. As known, there are productivity and cost efficiency concern in EUVL tool. Current state-of-art photo ArF 193 nm lithography has reached limited of half pitch 40 nm, self-aligned double patterning (SADP) has been chosen as compromised solution rather than EUVL.

SADP designs line to space (L/S) from control spacer thickness for pitch definition. To meet device's lower RC delay requirement, SADP not only needs consistent pitch but also higher patterning aspect ratio, which reminds hard mask material as higher etch selectivity and better dispersion absorption material. As Chiu (2008) reported, ArF dry was chosen to pattern on amorphous carbon (a-C) film stack. The resist pattern was transferred on a-C and following etch define pitch splitting. [1] SADP with extra hard mask of amorphous carbon is inserted in the bottom of conventional hard

mask. The purpose of a-C film is not only hard mark of etch stop but also excellent light dispersion absorption of pattern recognition. In Bencher and Chen's experiment (2008), it concluded that in SADP generic process flow, spacer doubled pattern density after stripping amorphous carbon as original template material. [2] However, SADP with amorphous carbon suffered severe pattern wiggling after last etch step. The toppling of a-C film in necking position induce SADP wiggling shown in Fig.1.

In this work we focused on a-C wiggling mechanism that addresses of charactering a-C material with Fourier transform infrared spectroscopy (FTIR) and semi-quantitating with dry etch rate. In Mahtani's research in 2010,  $sp^3$  ratio in FTIR represented diamond allotrope percentage and  $sp^2$  ratio represented graphite in amorphous carbon film property. [3,8] The  $sp^3/sp^2$  ratios of amorphous carbon showed different wiggling phenomenon after dry etch. In this paper,  $sp^3/sp^2$  ratios of amorphous carbon had proportional correlation with dry etch selectivity. The lowest amorphous carbon  $sp^3/sp^2$  ratios from FTIR gets the lowest etch selectivity in blanket and the highest line edge roughness (LER) value. Furthermore, with  $sp^3/sp^2$  ratios optimization, this significantly resulted in 3 times higher etch selectivity in blanket, 2.7 times lower LER and wiggling free in patterning.

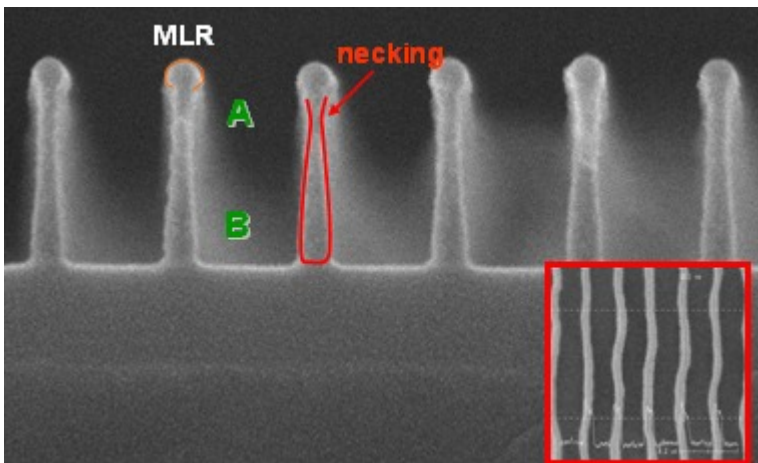


Fig.1 Wiggling mechanism, position A chemical side etching is more serious than the position B.

## 2. Experimental

### 2.1 Introduction of the SADP process flow

The schematic flow of the SADP process is shown in Fig. 2. Firstly, amorphous carbon (a-C) and MLR films were deposited on the poly-silicon as Hard Mask (HM) for following lithography process. The half-pitch of 56 nm was used for lithography patterning. Next, the photo-resist (PR) trimming and a-C core etching results in adequate core profile for sequential spacer deposition. A conformal spacer film was deposited onto the a-C core to develop a spacer HM for

another self-aligned patterning. And then, spacer dry etch back and a-C core removing by ASH is used to accomplish the SADP procedure which an equal 28 nm line and space CD can be achieved. As to the SADP process, we will focus on a-C core etching step (Step 3) modification for reducing line wiggling side effect.

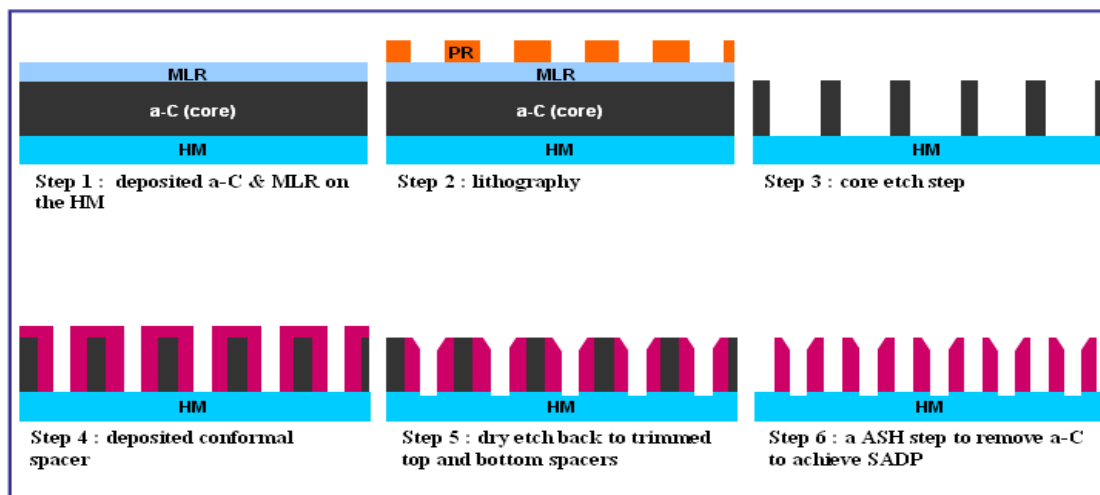


Fig 2. Schematic flow of the SADP process

## 2.2 Amorphous carbon (a-C) film deposition / etching / metrology method

For amorphous carbon material study, there are five different samples with 200nm thickness to be prepared. The detail process condition is in Table 1. As to the samples 1 and 2, a-C film was deposited by precursor  $C_2H_2$  gas in which uses the He and  $H_2$  as carrier gas with various process temperature, 300 and 550 °C by Company A system.[4,8,9] On the other hand, the HRF (13.56 MHz) and LRF (100 KHz) power to create the plasma were been used simultaneously. The different precursor  $C_3H_6$  gas with He or Ar carrier gas process by Company B system were utilized to samples 3-5 preparation, however only HRF power was applied. As to sample 3, the process temperature is 300 °C that is lower than that of samples 4-5, 550 °C. About the a-C HM etching, the process environment includes Ar,  $O_2$ , and  $N_2$  gas with Bias power by Lam system. Accordingly, the measurement of a-C thickness, stress, refractive index (RI), and extinction (k) values (633nm) were performed by KLA (FX200) system.

Sample	1	2	3	4	5(advance a-C)
System	Company A	Company A	Company B	Company B	Company B
Precursor	$C_2H_2$	$C_2H_2$	$C_3H_6$	$C_3H_6$	$C_3H_6$
Temperature	300°C	550°C	300°C	550°C	550°C
Carrier Gas	He, $H_2$	He, $H_2$	He, Ar	He	He, Ar
HRF power	open	open	open	open	open
LRF power	open	open	close	close	close

Table 1. The process condition for a-C films preparation.

### 2.3 FTIR measurement method

The chemical structure and quantitative composition analyses of the samples that is deposited on silicon substrate were performed by Fourier transform infrared spectroscopy (FT-IR) (Thermo ECO3000). Table 2 shows the absorption wavenumber and its comparative vibrational modes of the common a-C film [3]. Relying on the deposition conditions, the a-C film quality can vary from soft polymer-like a-C:H to hard diamond-like microstructure. The beneficial mechanical properties arise from  $SP^3$  bond carbon sites, while the optical and electronic properties are dependent on the  $SP^2$  carbon sites [5]. In this paper, we will determine the qualities of the various a-C films by the  $SP^2$ ,  $SP^3$ , and its ratio ( $SP^3/SP^2$ ) bonded carbon difference. The  $SP^3$  content is the sum of all the related bonding and the  $SP^2$  content is the same.

Wavenumber (cm-1)	Vibrational Mode Assignment
840	$Sp^2$ bonded $CH_2$ & $CH_3$ bending
885	$Sp^3$ C=C
990~1100	$CH_x$
1350~1450	C- $CH_x$
1600	$Sp^2$ -C=C
2850	$Sp^3$ $CH_3$
2920	$Sp^3$ $CH_2$ and CH
2950	$CH_2$ $Sp^2$
3050	$CH_x$ $Sp^2$

Table 2. Vibrational modes of molecular groups for common a-C film

## 3. Result and Discussion

### 3.1 FTIR / RI / Stress results

In our work, we suggested that a-C film was characterized with three main factors: refractive index (RI), stress and  $SP^3/SP^2$  bonding ratio in FTIR. Refractive index shows optical performance of material. Stress reveals modulus of liner elasticity of material under certain strain. And both of RI and stress were been measured with light source wavelength 633nm in KLA FX-2000. FTIR bonding represents material absorption arising with dispersing spectrum of vibration, scissor and stretching vibration. To semi-quantity of a-C samples, we distinguished particular molecular groups in FTIR spectrum. This is shown in Table 3, which each sample is prepared in thickness within  $200nm \pm 3.0\%$ . At first, refractive index (RI) of a-C optical property was decided by a-C process conditions.

Higher process temperature and variable process pressure in a-C process, even with different precursor, might get higher  $SP^2$  bonding intensity in FTIR. Sample 2 has been measured as the highest  $SP^2$  resulted in the highest RI. However, a-C optical property (RI) didn't reflect mechanical strength [6]. In this paper, a-C mechanical strength had

been ascertained as etch selectivity, and it will be explained later. Indeed, Fig.4 showed that the refractive index has no liner correlation with mechanical strength. Second, stress of a-C was decided by a-C process parameters. As shown in Table 3, samples 2 and 4 which with higher process temperature resulted in tensile stress but sample 5 showed compressive stress, alternatively. Samples 1, 3 and 5 with lower process temperature displayed compressive stress. Wu et al. [7] also mentioned the a-C film stress can't reflect the comparative mechanical strength.

Sample	Film property				FTIR			
	THK (A)	U%	RI (633)	Stress (GPa)	Sp <sup>2</sup>	C <sub>x</sub> H <sub>y</sub>	Sp <sup>3</sup>	SP <sup>3</sup> /SP <sup>2</sup> ratio
1	1904	1.7	1.890	-3.931	0.736	6.580	1.933	2.63
2	2147	1.5	2.021	0.1166	1.837	4.761	1.701	0.93
3	2049	1.6	1.875	-4.814	0.655	4.467	1.675	2.56
4	2122	2.8	1.861	0.891	0.764	5.534	1.698	2.22
5(Advance a-C)	2019	4.1	1.956	-3.620	0.563	5.473	1.730	3.07

Table 3. a-C film property and FTIR measurement result.

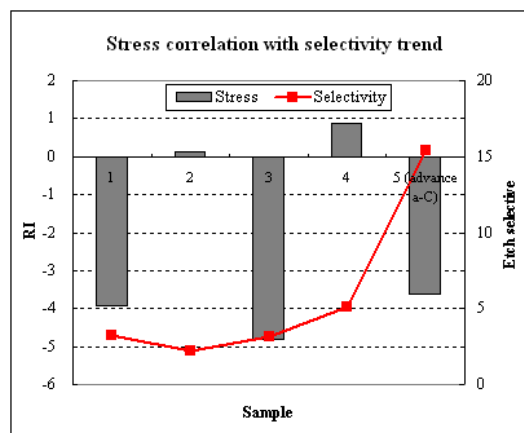
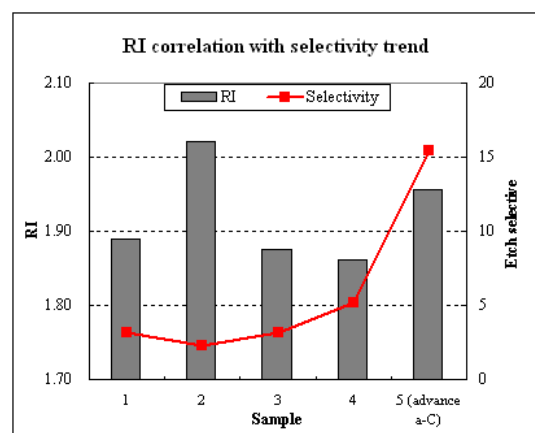


Fig 4(a). Correlation between RI and Etch selectivity.

Fig 4(b). Correlation between Stress and Etch selectivity.

### 3.2 Etch rate and etch selectivity results

Final, SP<sup>3</sup>/SP<sup>2</sup> bonding ratio in FTIR was decided by a-C process parameters. High SP<sup>3</sup>/SP<sup>2</sup> bonding ratio represents high percentage of diamond-like microstructure in entire a-C film and respective with hard mechanical strength as well. To semi-quantitatively determine, etch selectivity with different etch process conditions on blanket wafer was chosen in this paper. And etch selectivity had been defined as:

$$Etch - selectivity(\%) = \frac{Etch - Rate(etch - gas : O_2 base)}{Etch - Rate(etch - gas : CF_x base)} \dots \dots \text{formula (1)}$$

Etch Process	Control mode	Pressure	Gas
a-C etch	Time	10 mTorr	CO/O <sub>2</sub>

Table 4(a). Etch gas and etch process conditions in O<sub>2</sub> base.

Etch Process	Control mode	Pressure	Gas
TEOS etch	Time	30 mTorr	C <sub>4</sub> F <sub>8</sub> /Ar/O <sub>2</sub>

Table 4(b). Etch gas and etch process conditions in CF<sub>x</sub> base.

In Table 5, sample 1,3,4,5 has similar a-C etch rate that etch rate range is from 113.2 to 160.8 nm/min. However, the main particularly difference in sample 5 is its lowest oxide etch rate, 7.3 nm/min, on blanket wafer. In addition, sample 5 exhibited the highest etch selectivity (Fig 5). This result implied it has higher etch resistance comparing with other samples under dry etch process. In other words, sample 5 had better mechanical strength than other samples and this film characteristic can be correspond to the higher SP<sup>3</sup>/SP<sup>2</sup> ratios outcome.

Sample	SP <sup>3</sup> /SP <sup>2</sup> ratio	a-C E/R (nm/min)	Ox E/R (nm/min)	Etch selectivity
1	2.63	145.8	45.6	3.2
2	0.93	644.8	287.8	2.2
3	2.56	160.8	51.6	3.1
4	2.22	142.4	27.7	5.1
5(Advance a-C)	3.07	113.2	7.3	15.4

Table 5. a-C film etch selectivity and FTIR measurement

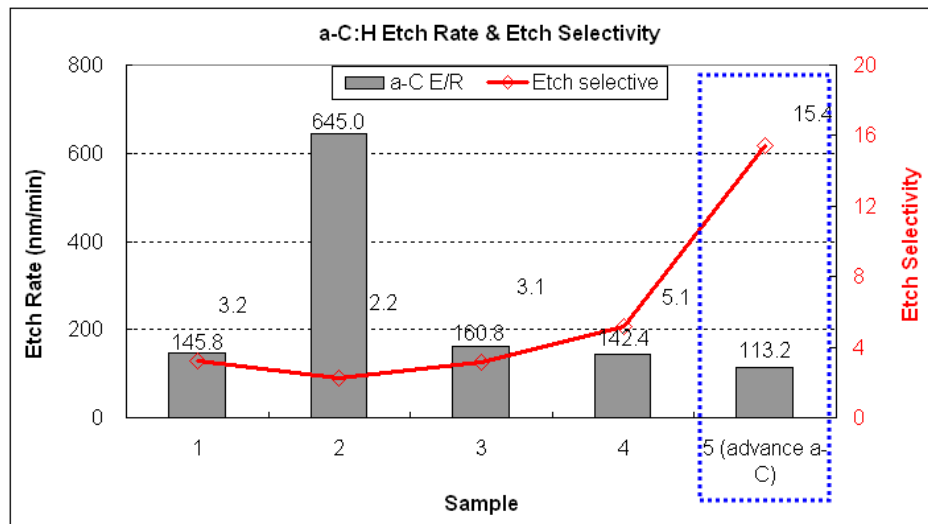


Fig. 5 a-C etch rate with O<sub>2</sub> base etch gas and etch selectivity.

### 3.3 LER measurements in SADP

Line edge roughness (LER) is one of the most concerns in SADP. Many reports had been known in improving LER performance. LER was getting more challenge in 3X and beyond. Our result suggested that LER performance can be improved from 7.5 to 5.3 nm (Table 6) with SP<sup>3</sup>/SP<sup>2</sup> ratios increase from 0.93 to (2.2~2.6) and etch selectivity increase from 2.2 to (3.1~5.1) on blanket. Server line wiggling appearance in sample 2 had been diminishing but not vanished. After a-C process optimization of sample 5, the highest SP<sup>3</sup>/SP<sup>2</sup> value of 3.07 and etch selectivity reported with 15.4 on blanket, had the lowest LER value of 2.7 nm. Therefore, it can be concluded that increasing a-C film mechanical strength has obviously improvement on LER performance in SADP process. Furthermore, this LER value of 2.7nm meets the ITRS current LER roadmap of gate length 32nm specifies 2.6 nm.

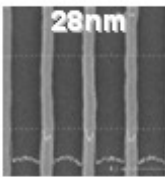
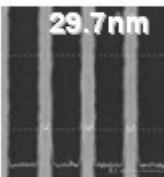
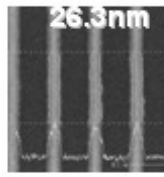
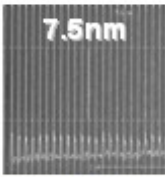
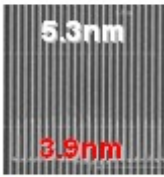
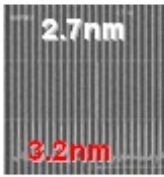
		Sample 2	Sample 1, 3, 4	Sample 5
AEI (nm)	ADI	50nm	44nm	42.7nm
	AEI			
	LER LWR			
LER comparison	XX	△	○○○	
SP <sup>3</sup> /SP <sup>2</sup> ratio	0.93	2.22~2.63	3.07	
a-C etch rate (nm/min)	645	142~160	113	
a-C etch selectivity	2.2	3.1~5.1	15.4	

Table 6. Different a-C samples resulted different LER / LWR after a-C etch

### 4. Conclusion

In this investigation, a-C film properties were discussed and correlated with SADP LER to indicate that the most important factor contributing to line wiggling is SP<sup>3</sup>/SP<sup>2</sup> bonding ratio in FTIR rather than refractive index and stress. With increasing SP<sup>3</sup>/SP<sup>2</sup> ratios in a-C, which might suggested that increasing percentage of diamond allotrope microstructure in a-C, had higher etch resistance, better LER and line wiggling free. To characterized a-C film on blanket, we suggested semi-quantitatively with etch selectivity. In this work, with increasing etch selectivity value up to 15.4; LER decreasing to 2.7nm; wiggling free reported in under half-pitch 42.7nm.

## Reference

1. M. C. Chiu, Benjamin Szu-Min Lin and M. F. Tsai, et al., "Challenges of 29nm Half-Pitch NAND FLASH STI Patterning with 193nm Dry Lithography and Self-Aligned Double Patterning", Proc, SPIE 7140-72 (2008)
2. Christopher Bencher, Yongmei Chen and Huixiong Dai, et al. "22nm Half-Pitch Patterning by CVD Spacer Self Alignment Double Patterning (SADP)", Proc. of SPIE Vol.6924 69244E (2008)
3. Pratih Mahtani, degree of Master thesis, "Optical and Structural Characterization of Amorphous Carbon Films", Department of Electrical and Computer Engineering University of Toronto(2010)
4. Gishun Hsu, Charles Merrill and Scott Stoddard, "Method for purifying acetylene gas for use in semiconductor processes", U.S. patent 7,820,556 B2, (2010)
5. J. Robertson, "Properties of diamond-like carbon", *Surf. Coat. Technol.* 50, 185 (1992).
6. Martin Glodde, Sebastian Engelmann and Michael Guillorn, et al. "Systematic Studies on Reactive Ion Etch-Induced Deformations of Organic Underlayers", Proc. of SPIE Vol. 7972 79716 (2011)
7. Qingguo Wu, James S. Sims and Mandyam Sriram, et al., "High compressive stress carbon liners for MOS devices", U.S. patent 7,906,817 B12, (2011)
8. Pramod Subramonium, Yongsik Yu and Zhiyuan Fang, et al., "Methods of depositing stable and hermetic ashable hardmask films", U.S. patent 7981777B1, (2011)
9. Pramod Subramonium, Zhiyuan Fang and Jon Henri, "Methods of depositing highly selective transparent ashable hardmask films", U.S. patent 7981810B1, (2011)